Supplementary Materials for

Observation of Significant Photosynthesis in Garden Cress and Cyanobacteria under Simulated Illumination from a K Dwarf Star

Vilović *et al.*
*Corresponding author. Email: iva.vilovic@campus.tu-berlin.de

This PDF file includes:

Supplementary Equations and Text
Figs. S1 to S3
Table S1

Supplementary Equations and Text

The hypothetical planet in this work orbits a ~4300 Kelvin Kdwarf star in the center of its habitable zone where it receives 0.6 times the solar constant (S_0). The planet's integrated top-of-the-atmosphere (TOA) flux ($F_{K,TOA}$) can therefore be written as:

$$F_{K,TOA} = 0.6 \cdot S_0 = 0.6 \cdot 1368\, W/m^2 = 820.8\, W/m^2. \tag{1}$$

We used the following parameters for further calculations:

$\sigma = 5.67... \cdot 10^{-8}$	$[W/m^2K^4]$	$Stefan - Boltzmann\ constant$
$d_{\odot,\text{⍰}} = 1 \cdot AU = 149.598 \cdot 10^{9}$	$[m]$	$astronomical\ unit;\ Sun - Earth\ distance$
$T_{\odot} = 5778$	$[K]$	$solar\ effective\ temperature$
$R_{\odot} = 6.96 \cdot 10^{8}$	$[m]$	$solar\ radius$
$M_{\odot} = 1.989 \cdot 10^{30}$	$[kg]$	$solar\ mass$
$L_{\odot} = 4\pi \cdot R_{\odot}^2 \cdot \sigma \cdot T_{\odot}^4 = 3.85... \cdot 10^{26}$	$[W]$	$solar\ luminosity$
$F_{\odot} = \sigma \cdot T_{\odot}^4 = 6.32... \cdot 10^{7}$	$[W/m^2/nm]$	$solar\ flux\ at\ stellar\ surface$
$S_0 = L_{\odot} / (4\pi \cdot AU^2) = 1368$	$[W/m^2]$	$integrated\ solar\ flux\ at\ Earth\ TOA$ $i.e.\ solar\ constant$

Calculating K dwarf stellar parameters

To obtain the effective temperature of the K dwarf star (T_K) we first integrated the K dwarf emission spectrum (F_K), and then used the Stefan-Boltzmann law rearranged for temperature:

$$T_K = \sqrt[4]{\frac{F_K}{\sigma}} = 4285\, K \tag{2}$$

We searched for a ~4300 K main-sequence star (~5 Gyr old) in the stellar evolution tracks ((Baraffe et al., 2015) in order to identify a stellar mass, radius and luminosity that would produce this effective temperature. We did a linear interpolation between a 3984 Kelvin star (T_1; with a stellar mass $M_1 = 0.6\, M_{\odot}$ and a stellar radius $R_1 = 0.562\, R_{\odot}$) and a 4430 Kelvin star (T_2; with a stellar mass $M_2 = 0.7\, M_{\odot}$ and a stellar radius $R_2 = 0.648\, R_{\odot}$) in order to obtain the target parameters.

$$T_1 = 3984\, K; \qquad T_2 = 4430\, K \tag{2.1}$$

$$M_1 = 0.6\, M_{\odot}; \qquad M_2 = 0.7\, M_{\odot} \tag{2.2}$$

$$R_1 = 0.562\, R_{\odot}; \qquad R_2 = 0.648\, R_{\odot} \tag{2.3}$$

Using T_K we computed the *weight* along the temperature scale:

$$weight = \frac{T_K - T_1}{T_2 - T_1} \tag{2.4}$$

We then used this *weight* along the mass and radius scales in order to calculate the mass (M_K) and radius (R_K) of the K dwarf star:

$$M_K = [M_1 + (M_2 - M_1) \cdot weight] \cdot M_\odot = 0.667\, M_\odot \tag{2.5}$$
$$R_K = [R_1 + (R_2 - R_1) \cdot weight] \cdot R_\odot = 0.620\, R_\odot \tag{2.6}$$

Using R_K we calculated the luminosity of the K dwarf:

$$L_K = 4\pi \cdot R_K^2 \cdot \sigma \cdot T_K^4 = 0.116\, L_\odot \tag{2.7}$$

Using this information, we calculated the distance *d* of the hypothetical planet to its host star where it receives 0.6 solar constants:

$$d = \sqrt{\frac{R_K^2 \cdot \sigma \cdot T_K^4}{F_{K,TOA}}} / AU = 0.441\, AU. \tag{2.8}$$

Calculating the modeled K dwarf spectrum at the planetary top-of-atmosphere

The wavelength resolved K dwarf flux at the stellar surface ($F_{K,nm}$) and its integrated flux (F_K) are proportional to their counterparts at the planetary TOA at a distance *d* from the host star. Using this proportionality, we obtained the wavelength resolved K dwarf flux at the planet's TOA ($F_{K,TOA,nm}$) at a distance d = 0.441 AU from the host K dwarf star:

$$\frac{F_{K,TOA,nm}}{F_{K,TOA}} = \frac{F_{K,nm}}{F_K} \quad \Rightarrow \quad F_{K,TOA,nm} = \frac{F_{K,nm} \cdot F_{K,TOA}}{F_K} = \frac{F_{K,nm} \cdot 0.6 \cdot S_0}{F_K}\,. \tag{3}$$

Calculating the modeled K dwarf spectrum at the planetary surface

The wavelength resolved flux received at the surface of the K dwarf planet ($F_{K,surf,nm}$) was calculated by multiplying the wavelength resolved TOA flux ($F_{K,TOA,nm}$) with the transmission (telluric) spectrum of Earth provided to us by Baker et al.(Baker et al., 2020). Their code wraps the *Planetary Spectrum Generator (*PSG) radiative transfer tool in order to calculate the Earth spectra and has a lower limit at 200 nm ((Villanueva et al., 2018). This transmission spectrum was calculated at zenith over Göttingen, Germany on a random fall day and reveals the composition of Earth's atmosphere, with its prominent water vapor absorption bands.

To simulate the change of the surface irradiation as a function of the star's position in the sky, it is necessary to simulate the change of the radiation as a function of time. We consider the star going through the zenith, i.e. that our hypothetical laboratory setup is near the planet's equator (latitude l = 0°). At night (for ~12 hours) there is no light; for the next 12 hours (starting at time t = 0), the radiation at the source evolves as per:

$$F(t) = F_{K,TOA} \cdot sin[\frac{t}{24\, hrs} \times 2\pi] = F_{K,TOA} \cdot sin[\frac{t}{12\, hrs} \times \pi] \tag{4}$$

For practicality reasons in the laboratory, we more simply averaged the daily dose of stellar illumination over half a sinusoidal cycle, i.e. calculated the average of sin (x) for $0 \le x \le \pi$:

$$\overline{sin(x)} = \frac{1}{\pi - 0}\int_0^\pi sin(x)dx = \frac{2}{\pi} = \sim 0.637 \tag{4.1}$$

The wavelength resolved surface flux ($F_{K,surf,nm}$) was then multiplied by the resulting factor 0.637 in order to obtain the daily averaged wavelength resolved surface spectrum for a 12 hour cycle ($F_{K,surf,avg}$). If we were to move the entire setup to a different planetary latitude, we would simply multiply our averaging factor with a cos (l) term. In the laboratory, this flux was then used in combination with an automatically implemented 12 hour day-night cycle.

Calculating the photosynthetic photon flux densities (PPFD)

The photosynthetic photon flux density (PPFD) is the total radiation produced by a light source within the photosynthetically active radiation (PAR; 400 – 700 nm) per unit area and time. The flux is expressed in units of μmol of photons $m^{-2}s^{-1}$. The energy of a photon is wavelength-dependent and can be expressed in Joules as:

$$E_{photon}\,(J) = h\cdot\nu = h\cdot\frac{c}{\lambda\,(nm)} = \sim\frac{1.9864\cdot 10^{-16}}{\lambda\,(nm)}, \tag{5}$$

where h is Planck's constant, and ν and λ are the photon's frequency and wavelength, respectively. The number of photons per unit area and time for a given wavelength can be calculated using the wavelength-distributed photon flux F_{photon}:

$$F_{photon} = \frac{W}{m^2 nm} = \frac{E_{photon}\,(J)}{m^2 s\,\lambda\,(nm)} \quad \rightarrow \quad \#_{photons}\left(\frac{1}{m^2 s\ \lambda\,(nm)}\right) = \frac{F_{photon}\left(\frac{1}{\lambda\,(nm)}\right)}{E_{photon}\left(\frac{1}{\lambda\,(nm)}\right)} \tag{5.1}$$

To obtain the wavelength resolved PPFD, i.e. the number of photons available for photosynthesis by primary producers within PAR per unit area, time and wavelength, the function above is divided by 6.022 $\cdot 10^{17}$ (i.e. by the value of 1 μmol):

$$PPFD\ (\mu mol_{photons}/m^2 s\,/\,nm) = \#_{photons}\left(\frac{1}{m^2 s\ \lambda\,(nm)}\right) / \,6.022\ \cdot\ 10^{17}. \tag{5.2}$$

We obtained the absolute PPFD value of the solar as well as K dwarf emission spectrum by integrating the wavelength resolved PPFD functions over the wavelength range 400 ≤ λ (nm) ≤ 700. This yields the following results:

- There are 512 μmol (photons) $m^{-2}s^{-1}$ available in modeled K dwarf PAR.
- There are 1446 μmol (photons) $m^{-2}s^{-1}$ available in modeled solar PAR.

The calculated solar PPFD value matches well with literature data for cloudless conditions ((Deo et al., 2022). When repeating the calculations for the simulated LED spectra, the results are as follows:

- There are 491 μmol (photons) $m^{-2}s^{-1}$ available in simulated K dwarf PAR.
- There are 1402 μmol (photons) $m^{-2}s^{-1}$ available in simulated solar PAR.

A graphical representation of the wavelength resolved PPFD of the high-resolution K dwarf and solar emission spectra as well as of the simulated LED spectra is shown in **Fig. S1.** For the experiments with cyanobacteria, which prefer a PAR intensity of 30–40 μmol (photons) $m^{-2}s^{-1}$, we decreased the wavelength-distributed flux of the modeled solar emission spectrum as well as its corresponding simulated LED spectrum by 48 times. To keep the original photonal ratio of the two spectral types, the K dwarf PAR intensity was decreased to 10 μmol (photons) $m^{-2}s^{-1}$.

Calculating the stellar energy inputs

We calculated the stellar energy input considered in the K dwarf and solar experiments (350 – 1500 nm) in comparison to the stellar energy input for the total available wavelength range of the PHOENIX library used to calculate the model spectra (50 – 5499 nm). We did this by integrating the PHOENIX spectra over the different wavelength ranges and subsequently computing their fractions.

- Sun: the stellar energy input considered (350 – 1500 nm) is 86.93%. The energy input not considered (i.e. 50 – 350 nm and 1500 – 5499 nm) is 13.07%.
- K dwarf: the stellar energy input considered (350 – 1500 nm) is 75.83%. The stellar energy input not considered (i.e. 50 – 350 nm and 1500 – 5499 nm) is 24.17%.

Therefore, more than 6/7 of the total solar and approximately 3/4 of the total K dwarf energy input are considered in this work.

Calculating the red to far-red photon flux ratios (R:FR)

The ratio of red to far-red light (R:FR) in a spectrum extensively influences the extension growth of a plant ((Holmes and Smith, 1977a, 1977b; Kusuma and Bugbee, 2021; Smth and Holmes, 1977). Plants use the pigment phytochrome, which exists in the red- (P_R) and far-red absorbing (P_{FR}) form, in order to perceive the quality of the light. The abundance of the pigments in each of the two forms is proportional to the amount of red and far-red light. A larger absorption of radiation by P_{FR} relative to P_R is associated with plant elongation including an increase in leaf size and stem length ((Kasperbauer, 1971; Kasperbauer and Peaslee, 1973; Kusuma and Bugbee, 2021). This is primarily used as a mechanism to compete with the neighboring canopy to optimize light capture. Recently, it has been proposed that taking an FR range of 730 ± 10 nm and an R range of 660 ± 10 nm is appropriate for the calculation of photon flux ratios ((Kusuma and Bugbee, 2021). Using these ranges, we calculated in *Python* a R:FR of **1.28 and 1.16 for the solar and K dwarf spectrum, respectively** (see **Table 1** in the main text).

Garden Cress: Pulse-Amplitude-Modulation fluorometer (PAM) signal scaling

In order to determine the optimal signal amplification (i.e. gain) and measuring light (ML) intensity for the PAM setting and get meaningful measurements of F_m and F_0 for our biological samples, we conducted a signal scaling experiment. We first established that 4 minutes and 30 seconds are needed between saturation pulses in order to obtain the same F_V/F_m value. We then proceeded to test ML intensities 1, 2, 4, 6, 8, 10 and 12 for gains 1 through 4 on a fully grown solar garden cress sample, each time noting the F_m, F_0 and F_V/F_m values. A plot of the F_m values against ML intensities for the four gains is shown in **Fig. S2**. The signal went off-scale at $F_0 \geq 620$ mV and $F_m \gtrsim 3200$ mV. Based on this sub-experiment, we chose the middle ground ML settings of gain = 2 and ML intensity = 8 for the garden cress experiments.

Fig. S1.

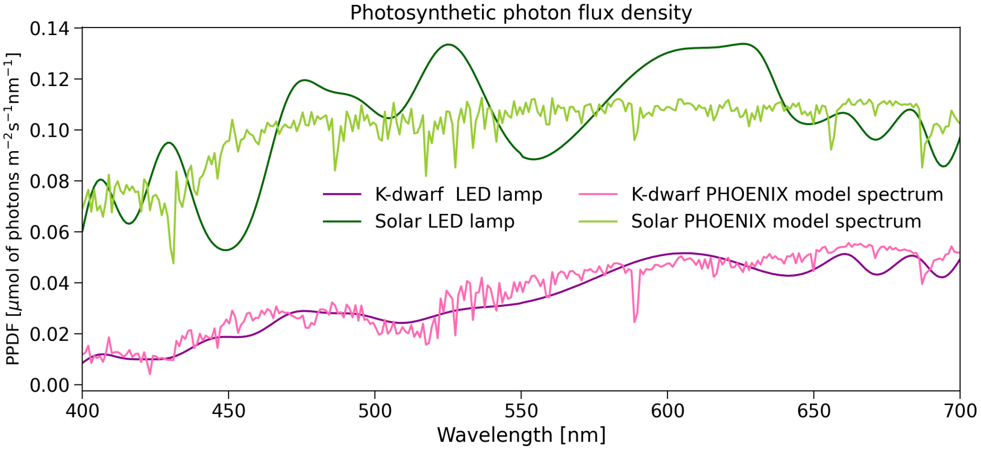

Wavelength resolved photosynthetic photon flux densities (PPFD) of modeled high-resolution K dwarf and solar emission spectra as well as of the simulated LED spectra. PPFD is expressed in units of µmol of photons per unit area (m^2), time (s) and wavelength (nm) and is obtained by dividing the wavelength resolved modeled K dwarf and solar emission spectra as well as the simulated LED spectra by the wavelength resolved photon energies within PAR (400 – 700 nm). Integrating the wavelength resolved PPFDs over the PAR range yields absolute PPFD values for K dwarf and solar radiation.

Fig. S2.

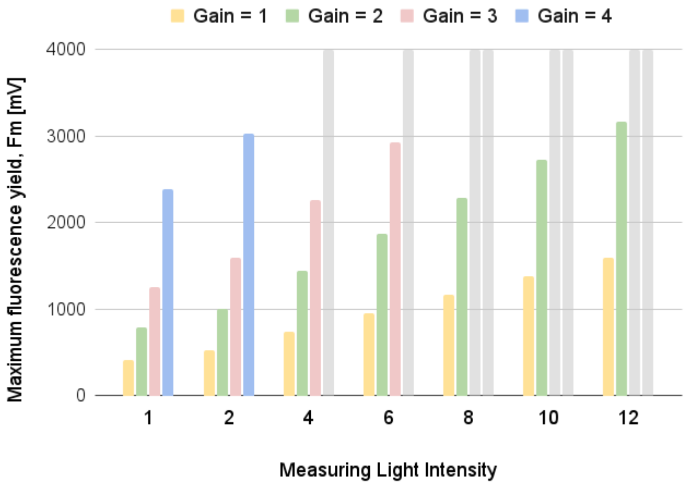

Results of the signal scaling experiment of the Mini-PAM II (Pulse-Amplitude-Modulation, Walz, Germany) on a fully grown solar sample of garden cress. Light-gray bars indicate signal saturation levels. Measuring light (ML) intensity setting 12 corresponds to 6000 µmol m^{-2} s^{-1} at a 7 mm fiber-optics-tip-to-sample-level distance and is adjusted at increments of 500 µmol m^{-2} s^{-1}. The chosen ML optimization is: Gain = 2; ML intensity = 8 for the garden cress experiment.

Fig. S3.

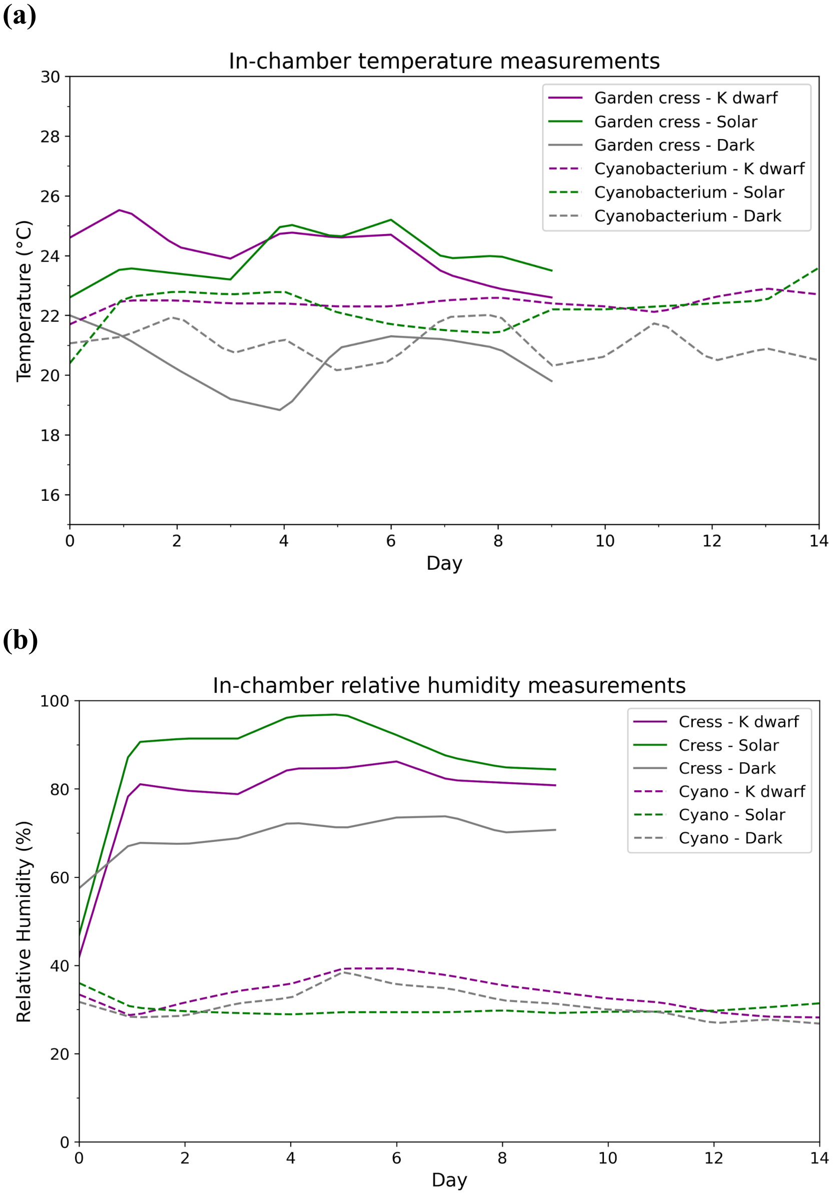

Temperature and relative humidity data in the experimental chamber recorded by a relative humidity and temperature sensor throughout experiments. (a) Tracked temperature data for the three radiation regimes (i.e. K dwarf radiation, solar radiation and dark conditions) during the experiments with garden cress (*Lepidium sativum*; experiment duration: 9 days) and cyanobacteria (*Chroococcidiopsis* sp. CCMEE 029; experiment duration: 14 days). (b) Corresponding relative humidity data.

Table S1.

Day	Garden cress			Cyanobacterium		
	Dry matter	Water content	Photosynthetic efficiency (via F_V/F_m)	Photosynthetic efficiency (via F_V/F_m)	Chlorophyll concentration (via F_0 ratio)	Culture growth (via integrated density)
0	–	–	–	**6.22×10^{-7}**	–	–
1	>0.05	>0.05	–	–	–	–
2	>0.05	>0.05	–	–	–	–
3	>0.05	>0.05	>0.05	**1.05×10^{-2}**	**0.042**	>0.05
4	>0.05	>0.05	>0.05	–	–	–
5	>0.05	>0.05	>0.05	**1.53×10^{-4}**	>0.05	>0.05
6	>0.05	>0.05	>0.05	–	–	–
7	>0.05	>0.05	>0.05	**1.17×10^{-6}**	**0.012**	>0.05
8	>0.05	>0.05	>0.05	–	–	–
9	>0.05	>0.05	>0.05	–	–	–
10	–	–	–	(saturation)	>0.05	>0.05
11	–	–	–	–	–	–
12	–	–	–	(saturation)	>0.05	>0.05
13	–	–	–	(saturation)	**0.022**	>0.05

p-values of statistical t-test. The test shows the statistical significance of the difference in mean values of each experimental test between K dwarf and solar radiation. A significance level of 0.05 (or 5%) is used. p-values below this threshold are considered statistically significant and are shown in bold.

References

Baker, A.D., Blake, C.H., Reiners, A., 2020. The IAG Solar Flux Atlas: Telluric Correction with a Semiempirical Model. ApJS 247, 24. https://doi.org/10.3847/1538-4365/ab6a1c

Baraffe, I., Homeier, D., Allard, F., Chabrier, G., 2015. New evolutionary models for pre-main sequence and main sequence low-mass stars down to the hydrogen-burning limit. Astron. Astrophys. Suppl. Ser.

Deo, R.C., Grant, R.H., Webb, A., Ghimire, S., Igoe, D.P., Downs, N.J., Al-Musaylh, M.S., Parisi, A.V., Soar, J., 2022. Forecasting solar photosynthetic photon flux density under cloud cover effects: novel predictive model using convolutional neural network integrated with long short-term memory network. Stoch. Environ. Res. Risk Assess. 36, 3183–3220. https://doi.org/10.1007/s00477-022-02188-0

Holmes, M.G., Smith, H., 1977a. The function of phytochrome in the natural environment—i. Characterization of daylight for studies in photomorphogenesis and photoperiodism. Photochem. Photobiol. 25, 533–538. https://doi.org/10.1111/j.1751-1097.1977.tb09124.x

Holmes, M.G., Smith, H., 1977b. The function of phytochrome in the natural environment—ii. The influence of vegetation canopies on the spectral energy distribution of natural daylight. Photochem. Photobiol. 25, 539–545. https://doi.org/10.1111/j.1751-1097.1977.tb09125.x

Kasperbauer, M.J., 1971. Spectral Distribution of Light in a Tobacco Canopy and Effects of End-of-Day Light Quality on Growth and Development. Plant Physiol. 47, 775–778. https://doi.org/10.1104/pp.47.6.775

Kasperbauer, M.J., Peaslee, D.E., 1973. Morphology and Photosynthetic Efficiency of Tobacco Leaves That Received End-of-Day Red and Far Red Light during Development. Plant Physiol. 52, 440–442. https://doi.org/10.1104/pp.52.5.440

Kusuma, P., Bugbee, B., 2021. Far-red Fraction: An Improved Metric for Characterizing Phytochrome Effects on Morphology. J. Am. Soc. Hortic. Sci. 146, 3–13. https://doi.org/10.21273/JASHS05002-20

Smth, H., Holmes, M.G., 1977. The function of phytochrome in the natural environment—iii. Measurement and calculation of phytochrome photoequilibria. Photochem. Photobiol. 25, 547–550. https://doi.org/10.1111/j.1751-1097.1977.tb09126.x

Villanueva, G.L., Smith, Protopapa, S., Faggi, S., Mandell, A.M., 2018. Planetary Spectrum Generator: An accurate online radiative transfer suite for atmospheres, comets, small bodies and exoplanets. J. Quant. Spectrosc. Radiat. Transf. 217, 86–104. https://doi.org/10.1016/j.jqsrt.2018.05.023